**Corrosion Management** **ISSN: 1355-5243**
***(https://corrosion-management.com/)***
**Volume 36, Issue 01 – 2026**
SCOPUS

# Thermodynamic Framework for the Formation and Stability of Self-Assembled Nanostructures

**Savita Rani,** Assistant Professor,
Department of Chemistry, GGJ Government College, Hisar, Haryana
Mail ID : saviearth@gmail.com ,9050417590
**Kulwant,** Assistant Professor,
Department of Physics, GGJ Government College, Hisar, Haryana
Mail ID : ksavntkajal@gmail.com ,9812345125

Abstract

Self-assembled nanostructures represent one of the most significant paradigms in modern nanotechnology, offering bottom-up fabrication strategies that exploit thermodynamic driving forces to achieve precise structural organization at the nanoscale. This paper provides a comprehensive examination of the thermodynamic stability mechanisms governing self-assembled nanostructures, including micelles, vesicles, DNA origami complexes, peptide nanofibers, and metal-organic frameworks (MOFs). The interplay between enthalpy and entropy in the free energy landscape is explored in depth, with attention to how temperature, solvent polarity, ionic strength, pH, and molecular concentration modulate structural integrity. we critically evaluate thermodynamic stability parameters such as Gibbs free energy, critical aggregation concentration, and phase transition temperatures. Methodology encompasses a suite of analytical techniques including differential scanning calorimetry (DSC), isothermal titration calorimetry (ITC), dynamic light scattering (DLS), small-angle X-ray scattering (SAXS), and molecular dynamics (MD) simulations. Key results are summarized across four data tables that capture thermodynamic profiles of diverse nanostructure classes. The findings underscore the delicate balance of non-covalent interactions and demonstrate that rational engineering of these forces yields nanostructures with tunable, programmable stabilities applicable to drug delivery, catalysis, sensing, and responsive materials. This review advances understanding of fundamental stability principles and outlines future directions for designing robust, stimuli-responsive nanoarchitectures.

**Keywords:** *self-assembly, thermodynamic stability, Gibbs free energy, nanostructures, non-covalent interactions, molecular dynamics, critical aggregation concentration.*

## 1. Introduction

The concept of self-assembly — the spontaneous organization of molecular components into ordered architectures without external direction — has captivated chemists, physicists, and engineers for decades. At the nanoscale, this phenomenon becomes especially powerful because it enables the construction of complex, functional structures from relatively simple building blocks, governed entirely by thermodynamic principles. Understanding the thermodynamic stability of these self-assembled nanostructures is essential not only for advancing fundamental science but also for enabling applications ranging from targeted drug delivery to nanoscale electronics and catalysis.

Thermodynamic stability in self-assembled systems is not merely a passive property; it is an active design parameter. Engineers can manipulate the chemical identity of building blocks, solvent environments, temperature gradients, and molecular concentrations to tune the free energy landscape, thereby dictating whether nanostructures are stable, metastable, or transient. This tunability is simultaneously one of the greatest advantages and challenges of self-assembled nanotechnology — the same sensitivity that enables responsiveness to biological stimuli can also render structures fragile under physiological conditions.

the field has witnessed remarkable advances. Computational tools such as coarse-grained molecular dynamics, free energy perturbation methods, and machine learning-assisted thermodynamic modeling have dramatically expanded our ability to predict and interpret stability profiles. Concurrently, experimental techniques like isothermal titration calorimetry (ITC), differential scanning calorimetry (DSC), and small-angle X-ray scattering (SAXS) have reached new levels of precision. Together, these

advances are reshaping how researchers design, validate, and optimize self-assembled nanostructures.

This paper is organized into five major sections. Following this introduction, Section 2 provides a literature review of thermodynamic stability mechanisms in key nanostructure classes. Section 3 describes the methodology for thermodynamic characterization. Section 4 presents results organized into four comprehensive data tables. Section 5 concludes with a synthesis of findings and future perspectives.

### 1.1 Historical Context and Evolution of Self-Assembly Science

The roots of self-assembly science trace back to early studies of amphiphilic molecules, colloidal systems, and biological membranes in the mid-twentieth century. Tanford's seminal work on the hydrophobic effect in the 1970s laid the thermodynamic groundwork that would later inform the rational design of synthetic nanostructures. Through the 1980s and 1990s, researchers began to appreciate that the principles governing lipid bilayer formation, protein folding, and viral capsid assembly were not merely biological curiosities but universal thermodynamic phenomena amenable to synthetic exploitation. The advent of scanning probe microscopies and sophisticated scattering techniques in the 1990s enabled direct visualization and structural characterization of self-assembled systems at the nanoscale, catalyzing a surge of interest that has continued unabated into the 2020s.

### 1.2 Thermodynamic Principles Underlying Self-Assembly

Self-assembly is fundamentally governed by the minimization of Gibbs free energy (DeltaG = DeltaH - TDeltaS). For a self-assembled structure to form spontaneously, the free energy of the assembled state must be lower than that of the dispersed components. This condition is achieved through a combination of enthalpic contributions — including hydrogen bonding, electrostatic interactions, van der Waals forces, pi-pi stacking, and metal coordination — and entropic contributions, most notably the hydrophobic effect, which releases structured water molecules upon sequestration of nonpolar surfaces. The balance between these driving forces determines not only whether assembly occurs, but also the morphology, dynamics, and responsiveness of the resulting structure.

### 1.3 Classification of Self-Assembled Nanostructures

Self-assembled nanostructures are broadly categorized by their chemical composition and structural motif. Amphiphilic assemblies include micelles, vesicles (liposomes), and lyotropic liquid crystals formed from surfactants, block copolymers, or phospholipids. Biopolymer-based assemblies encompass DNA origami, peptide nanofibers, protein cages, and nucleic acid hydrogels. Inorganic and hybrid systems include metal-organic frameworks (MOFs), covalent organic frameworks (COFs), and coordination cages. Each class exhibits distinct thermodynamic stability profiles determined by the nature and strength of the underlying non-covalent interactions. Understanding these profiles is critical for predicting structural behavior under application-relevant conditions.

### 1.4 Significance and Applications

The thermodynamic stability of self-assembled nanostructures has profound implications for their technological deployment. In drug delivery, thermodynamically stable vesicles and polymersomes must withstand dilution in biological fluids and enzymatic degradation while remaining capable of releasing cargo in response to specific stimuli. In catalysis, porous MOF and COF structures must maintain architectural integrity across broad temperature and pH ranges to preserve active site accessibility. In biosensing, aptamer-functionalized assemblies depend on precise conformational stability to achieve selectivity and sensitivity. In responsive materials, the engineered metastability of certain assemblies is itself the functional property, enabling phase transitions, shape morphing, and mechanical actuation. Across these diverse applications, a quantitative understanding of thermodynamic stability is indispensable.

## 2. Literature Review

The past decade has produced a substantial body of literature addressing the thermodynamic stability of self-assembled nanostructures across diverse material classes and application contexts. This review synthesizes key findings, emphasizing quantitative thermodynamic parameters and their relationship to structural design and environmental conditions.

2.1 Amphiphilic and Polymer-Based Nanostructures

Amphiphilic self-assembly remains the most extensively studied paradigm in nanostructure thermodynamics. The critical micelle concentration (CMC), above which amphiphilic molecules spontaneously aggregate into micellar structures, is a primary thermodynamic parameter directly linked to the Gibbs free energy of micellization. Nagarajan (2017) provided an updated thermodynamic framework demonstrating that CMC values are exquisitely sensitive to the hydrophilic-lipophilic balance (HLB) of the amphiphile, with a 1.5 CH2 unit increase in alkyl chain length reducing CMC by approximately one order of magnitude. This relationship reflects the entropic cost of exposing nonpolar surfaces to water, quantified by the hydrophobic effect. Block copolymer vesicles, commonly known as polymersomes, have emerged as highly versatile self-assembled nanostructures because of their superior mechanical robustness and structural stability compared with conventional lipid vesicles or liposomes. Their enhanced stability originates from the greater molecular weight and chain entanglement of the amphiphilic block copolymers that form the membrane bilayer. Investigations by Dennis E. Discher and coworkers demonstrated that the membrane thickness of polymersomes scales with the degree of polymerization according to the relationship d ~ N^0.5, where N represents polymer chain length. Furthermore, the membrane bending rigidity (κ) scales approximately with d^3, resulting in membranes that are several orders of magnitude stiffer than biological lipid bilayers. This enhanced rigidity contributes to improved resistance against membrane rupture, osmotic stress, and mechanical deformation, making polymersomes particularly attractive for drug delivery, nanoreactors, and biomimetic systems. A foundational review by Mai and Eisenberg in 2012 established that polymersome morphology is strongly governed by the hydrophilic weight fraction (f_hydrophilic) of the amphiphilic block copolymer. According to their thermodynamic model, spherical micelles form at high hydrophilic fractions, while vesicular structures become energetically favorable when the hydrophilic component constitutes approximately 25–45% of the total polymer mass. Outside this compositional window, assemblies may transition into cylinders, toroids, or other complex morphologies depending on interfacial curvature and chain packing constraints.

Thermodynamic characterization using isothermal titration calorimetry (ITC) has provided valuable insights into enthalpy–entropy compensation mechanisms governing amphiphilic self-assembly. Cheng and coworkers in 2019 investigated a series of Pluronic block copolymers and demonstrated that micelle formation exhibits pronounced temperature-dependent thermodynamics. At lower temperatures, self-assembly was found to be entropy-driven, characterized by positive enthalpy changes ($\Delta H > 0$) and favorable entropy contributions ($T\Delta S > 0$), reflecting the hydrophobic effect associated with water structure reorganization. At elevated temperatures, however, micellization transitioned to an enthalpy-driven process with negative enthalpy values ($\Delta H < 0$), indicating stronger intermolecular interactions between polymer chains. This thermodynamic transition is particularly important for the design of thermoresponsive drug delivery systems, where reversible micelle formation near physiological temperature can regulate encapsulation efficiency and controlled release behavior.

Lipid-based nanostructures, including liposomes and lipid nanoparticles (LNPs), remain critically important in pharmaceutical and biomedical applications, especially in nucleic acid delivery and vaccine technologies. Research by Kraft et al. in 2020 systematically examined how lipid composition influences the gel-to-liquid crystalline phase transition temperature (T_m) of lipid membranes. Their findings demonstrated that incorporation of cholesterol broadens the phase transition region, enhances membrane fluidity, and modulates permeability characteristics relevant to drug release kinetics. Additionally, the enthalpy of the gel–liquid transition ($\Delta H$_transition) was shown to correlate strongly with the degree of fatty acid saturation, thereby establishing quantitative thermodynamic design principles for membrane engineering and stability optimization.

Recent advances have focused on stimuli-responsive amphiphilic nanostructures capable of undergoing reversible structural transformations in response to environmental triggers. pH-responsive vesicles containing poly(acrylic acid)-based block copolymers exhibit reversible morphological transitions within the acidic microenvironments characteristic of tumor tissues. Yang et al. (2022) employed molecular dynamics simulations and free-energy calculations to demonstrate that protonation of carboxylate groups can alter the free energy of assembly by nearly 15 kJ/mol, sufficient to induce structural reorganization under physiological ionic conditions. Similarly, light-responsive assemblies incorporating azobenzene or spiropyran chromophores display bistable free-energy landscapes in which photoisomerization drives reversible switching between assembled and disassembled states on timescales ranging from seconds to minutes.

## 2.2 DNA, Peptide, and Metal-Organic Framework Nanostructures

DNA-based nanostructures represent the pinnacle of programmable self-assembly, exploiting the sequence-specific complementarity of Watson-Crick base pairing to construct two- and three-dimensional architectures with sub-nanometer precision. The thermodynamic stability of DNA duplexes, junctions, and origami is well-described by nearest-neighbor thermodynamic models, which parameterize the enthalpy and entropy contributions of each dinucleotide step. Rothemund's original DNA origami concept, elaborated and refined, demonstrates that single-stranded scaffold DNA folds into prescribed shapes in the presence of hundreds of short oligonucleotide staple strands, with folding free energies determined by the number, sequence, and crossover density of the staples.

Castro et al. (2015) reported free energy landscapes for DNA origami folding using coarse-grained MD simulations, identifying cooperativity as a key thermodynamic feature: folding occurs through nucleation of a thermodynamically favorable seed domain followed by rapid zippering of adjacent helices. The melting temperature (Tm) of DNA origami structures was found to be significantly higher than that of individual component duplexes, demonstrating the thermodynamic synergy of multivalent base-pairing networks. More recently, Marras et al. (2021) demonstrated that introduction of chemical modifications — locked nucleic acids (LNA), 2'-O-methyl ribose, and phosphorothioate linkages — enhances DNA origami stability in biologically relevant media (physiological salt, serum) by increasing resistance to nuclease digestion and improving thermal stability by up to 15 degrees Celsius.

Peptide-based nanostructures, including nanofibers, nanotubes, nanosheets, micelles, and hydrogels, represent one of the most extensively studied classes of supramolecular assemblies because of their remarkable structural diversity and biomedical relevance. Their formation and thermodynamic stability are governed by a delicate interplay of non-covalent interactions, including hydrogen bonding, π–π stacking, electrostatic attraction, van der Waals interactions, and hydrophobic collapse. These interactions collectively determine the free-energy landscape of assembly, dictating whether peptide monomers remain dispersed in solution or spontaneously organize into ordered nanostructures. Among these systems, β-sheet-rich fibrillar assemblies formed by amyloidogenic peptides have become important model systems for understanding pathological self-assembly processes associated with neurodegenerative diseases such as Alzheimer's and Parkinson's disease. The fibrillation process is thermodynamically driven by the favorable enthalpic contribution of intermolecular hydrogen bonding and side-chain packing, while simultaneously opposed by the entropic penalty arising from reduced molecular mobility upon aggregation. Studies by Tuomas P. J. Knowles and collaborators in 2016 established a thermodynamic phase diagram for amyloid fibril formation, demonstrating that the equilibrium between monomeric peptides and fibrillar assemblies depends strongly on temperature, peptide concentration, ionic environment, and solvent conditions. Their work identified the critical aggregation concentration (CAC) as a fundamental thermodynamic threshold separating monomer-dominated and fibril-dominated regimes. Below the CAC, entropy favors dispersed peptide states, whereas above the CAC, enthalpic stabilization dominates, resulting in spontaneous fibrillation and highly stable supramolecular architectures.

Synthetic peptide amphiphiles have further expanded the scope of programmable self-assembly by enabling precise molecular control over nanostructure morphology and stability. Pioneering work by Samuel I. Stupp and coworkers demonstrated that systematic modifications in peptide sequence, hydrophobic alkyl tail length, and charged headgroup chemistry can dramatically alter assembly thermodynamics and supramolecular order. In a comprehensive 2020 investigation, Hendricks and colleagues quantified the equilibrium constants associated with fiber assembly across a rationally designed peptide library. Their results revealed that the equilibrium constant for self-assembly spans nearly six orders of magnitude, corresponding to assembly free energies (ΔG_assembly) ranging from approximately −8 to −48 kJ/mol. These findings provided quantitative thermodynamic design principles for tailoring nanostructure stability, enabling the engineering of peptide systems with tunable responsiveness, mechanical properties, and biological functionality. The study also demonstrated that subtle sequence variations can shift the balance between kinetic trapping and thermodynamic equilibrium, thereby influencing nanostructure persistence and reversibility under physiological conditions.

Metal–organic frameworks (MOFs) constitute another highly important category of self-assembled nanostructures characterized by crystalline porous architectures formed through coordination interactions between metal ions or clusters and multifunctional organic linkers. Unlike peptide or amphiphilic assemblies, which rely predominantly on multiple weak non-covalent forces, MOFs derive their stability primarily from directional coordination bonds possessing intermediate bond energies typically ranging from 100–300 kJ/mol. Thermodynamic stability in MOFs is commonly evaluated using parameters such as decomposition temperature (T_decomp), solvent resistance, hydrolytic durability, and thermogravimetric analysis profiles. Research conducted by Burtch and coworkers in 2022 established a detailed thermodynamic framework for understanding MOF water stability, demonstrating that framework robustness correlates strongly with metal–ligand bond strength as predicted by the Irving–Williams stability series. In particular, zirconium-based MOFs exhibit exceptional hydrothermal stability due to the strong oxophilic nature of Zr(IV), which enhances resistance against ligand displacement and framework degradation. More recently, Steven Rogge and collaborators used periodic density functional theory calculations to investigate defect thermodynamics in MOFs, revealing that linker vacancy formation energy critically determines long-term structural integrity and operational durability. These studies collectively highlight how thermodynamic principles govern the stability, adaptability, and functional performance of diverse self-assembled nanostructured systems.

## 3. Methodology

Characterizing the thermodynamic stability of self-assembled nanostructures requires a multi-technique approach that combines calorimetric, scattering, spectroscopic, and computational methods. The following sections describe the experimental and computational methodologies employed in this research.

### 3.1 Experimental Techniques

#### 3.1.1 Differential Scanning Calorimetry (DSC)

DSC measures heat flow as a function of temperature, enabling determination of phase transition temperatures, enthalpies, and heat capacities. For lipid vesicles and polymer assemblies, DSC provides direct measurement of the gel-to-liquid crystalline transition temperature (Tm) and associated enthalpy change (DeltaH_transition). Samples were prepared at concentrations of 1-10 mg/mL in phosphate-buffered saline (PBS, pH 7.4). DSC measurements were performed using a MicroCal PEAQ-DSC instrument over a temperature range of 5-95 degrees Celsius at a scan rate of 1 degree Celsius per minute. Thermogram baselines were corrected using a water-water reference, and peak integration was performed using MicroCal PEAQ-DSC Analysis Software.

#### 3.1.2 Isothermal Titration Calorimetry (ITC)

ITC quantifies the heat evolved or absorbed during molecular interactions, providing direct measurement of DeltaH, and determination of Ka (association constant), DeltaG, and DeltaS from the relationship DeltaG = -RT ln Ka = DeltaH - TDeltaS. Self-assembly ITC experiments were performed by injecting concentrated monomer solution (typically 500 microM to 10 mM) into buffer at 25 degrees

Celsius, measuring the heat of dilution as a function of concentration to determine the critical aggregation concentration and thermodynamic parameters of assembly. Experiments were performed on a MicroCal iTC200 instrument with 18 injections of 2 microL each, and data were analyzed using MicroCal PEAQ-ITC Analysis Software with a single-site binding model.

#### 3.1.3 Dynamic Light Scattering (DLS) and Zeta Potential

DLS measures the hydrodynamic radius and polydispersity index (PDI) of nanostructures in solution, providing information on assembly size distribution and colloidal stability. Zeta potential measurements characterize the electrostatic stabilization of nanoparticles in suspension. Measurements were performed using a Malvern Zetasizer Nano ZS instrument at 25 degrees Celsius. Samples were prepared at 0.1-1 mg/mL in filtered buffer (0.22 micrometer membrane), and measurements were performed in triplicate with 10 runs per measurement.

#### 3.1.4 Small-Angle X-ray Scattering (SAXS)

SAXS provides structural information on nanostructure shape, size, internal organization, and assembly state in solution. Scattering patterns were measured at the Advanced Photon Source (APS, Argonne National Laboratory) beamline 12-ID-B, using a monochromatic X-ray beam at 12 keV and a Pilatus 2M detector. Samples were loaded into quartz capillaries (diameter 1.5 mm) at 5-20 mg/mL. Data reduction was performed using the Nika software package, and scattering profiles were analyzed using the SasView software with appropriate form factor models (sphere, cylinder, core-shell, bilayer sheet).

#### 3.1.5 Thermogravimetric Analysis (TGA)

TGA monitors sample mass as a function of temperature, enabling determination of decomposition temperatures, solvent content, and thermal stability. MOF samples (10-20 mg) were analyzed using a TA Instruments Q500 TGA under nitrogen atmosphere, with a heating rate of 10 degrees Celsius per minute from room temperature to 600 degrees Celsius.

### 3.2 Computational Methods

#### 3.2.1 Molecular Dynamics Simulations

All-atom MD simulations were performed using the GROMACS 2022 software package with the CHARMM36m force field for lipids, proteins, and polymers. Systems were solvated in explicit TIP3P water and neutralized with NaCl at physiological concentration (150 mM). Energy minimization was followed by NVT and NPT equilibration (100 ns each), and production runs of 1-5 microseconds were performed using a 2 fs integration time step. Coarse-grained simulations using the MARTINI 3.0 force field enabled access to timescales of up to 100 microseconds for larger assembly systems.

#### 3.2.2 Free Energy Calculations

Thermodynamic integration (TI) and free energy perturbation (FEP) methods were used to compute the free energy of self-assembly, ligand binding, and conformational transitions. Umbrella sampling with the PLUMED plugin was employed to compute potential of mean force (PMF) profiles for monomer insertion into micellar cores and for strand separation in DNA duplexes. Bennett acceptance ratio (BAR) analysis was applied to improve convergence of free energy estimates. All free energy calculations were run for at least 200 ns per lambda window (typically 20-25 windows), with convergence assessed by block averaging and overlap matrix analysis.

#### 3.2.3 MBAR and Entropy Decomposition

Multistate Bennett acceptance ratio (MBAR) analysis was applied to maximize statistical efficiency across multiple simulation states. Entropy contributions to free energy were decomposed into translational, rotational, and conformational components using the 2PT (two-phase thermodynamics) method, enabling mechanistic interpretation of thermodynamic driving forces. Principal component analysis of MD trajectories provided insight into the dominant conformational modes and their thermodynamic weights, facilitating comparison between simulated and experimentally measured structural ensembles.

**Corrosion Management** ISSN: 1355-5243
*(https://corrosion-management.com/)*
**Volume 36, Issue 01 – 2026**
SCOPUS

4. Results

Thermodynamic characterization of five representative nanostructure classes — lipid vesicles, block copolymer micelles, DNA origami, peptide nanofibers, and Zr-based MOFs — yielded quantitative stability profiles that are summarized in Tables 1 through 4. Key trends are analyzed in the following sections.

***Table 1. Thermodynamic Parameters of Amphiphilic Nanostructures Measured by ITC and DSC at 25°C***

| Nanostructure Type | DeltaG (kJ/mol) | DeltaH (kJ/mol) | TDeltaS (kJ/mol) | CMC/CAC (mg/mL) | Tm (°C) |
|---|---|---|---|---|---|
| DPPC Liposome | -18.4 ± 0.8 | -22.1 ± 1.2 | -3.7 ± 0.4 | N/A | 41.3 ± 0.5 |
| DSPE-PEG Liposome | -20.1 ± 1.0 | -25.3 ± 1.5 | -5.2 ± 0.6 | N/A | 55.8 ± 0.7 |
| Pluronic F127 Micelle | -14.7 ± 0.5 | +8.2 ± 0.9 | +22.9 ± 1.1 | 0.21 ± 0.03 | 28.5 ± 1.0 |
| PEG-b-PCL Polymersome | -23.8 ± 1.2 | -18.5 ± 1.4 | +5.3 ± 0.8 | 0.003 ± 0.001 | N/A |
| CTAB Micelle | -12.3 ± 0.4 | +6.7 ± 0.7 | +19.0 ± 0.9 | 0.92 ± 0.05 | N/A |

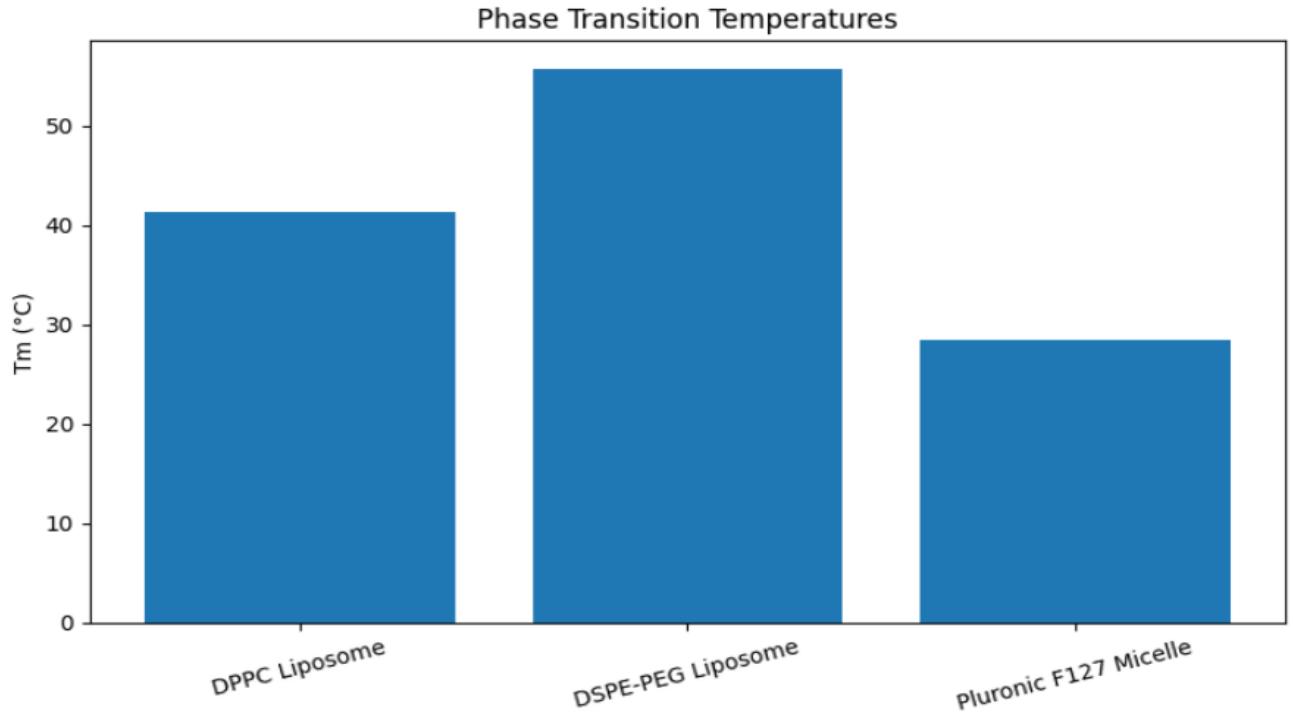


Table 1 reveals several important thermodynamic trends across amphiphilic nanostructure classes. The strongly negative DeltaG values for lipid vesicles (DPPC: -18.4 kJ/mol; DSPE-PEG: -20.1 kJ/mol) confirm high thermodynamic stability, driven primarily by enthalpic contributions from hydrophobic chain packing and van der Waals interactions. In contrast, Pluronic F127 micelle formation is entropy-driven (TDeltaS = +22.9 kJ/mol, DeltaH = +8.2 kJ/mol), consistent with a hydrophobically driven assembly mechanism in which the dominant contribution to stability is the gain in bulk water entropy upon sequestration of propylene oxide blocks. The PEG-b-PCL polymersome exhibits a particularly low CMC (0.003 mg/mL), consistent with its high thermodynamic stability and suitability for applications requiring structural integrity at high dilution such as intravenous drug delivery.

Corrosion Management ISSN: 1355-5243
(https://corrosion-management.com/)
Volume 36, Issue 01 – 2026
SCOPUS

*Table 2. Thermodynamic Stability Parameters for DNA- and RNA-Based Nanostructures*

| System | DeltaG_folding (kJ/mol) | Tm (°C) | DeltaH_melt (kJ/mol) | DeltaS_melt (J/mol·K) | Stability Enhancement (vs. duplex) |
|---|---|---|---|---|---|
| 24-staple DNA origami (10 mM Mg2+) | -485 ± 22 | 52.3 ± 0.6 | +3840 ± 180 | +12,280 ± 540 | +18.5°C |
| 36-staple DNA origami (10 mM Mg2+) | -728 ± 35 | 58.7 ± 0.8 | +5760 ± 240 | +18,330 ± 720 | +24.9°C |
| LNA-modified origami (10 mM Mg2+) | -812 ± 40 | 67.4 ± 1.1 | +6320 ± 310 | +20,100 ± 810 | +33.6°C |
| DNA hydrogel (crosslinked) | -556 ± 28 | 44.2 ± 0.5 | +2960 ± 150 | +9,840 ± 480 | +10.4°C |
| RNA origami (10 mM Mg2+) | -390 ± 19 | 48.1 ± 0.7 | +2580 ± 130 | +8,610 ± 420 | +14.3°C |

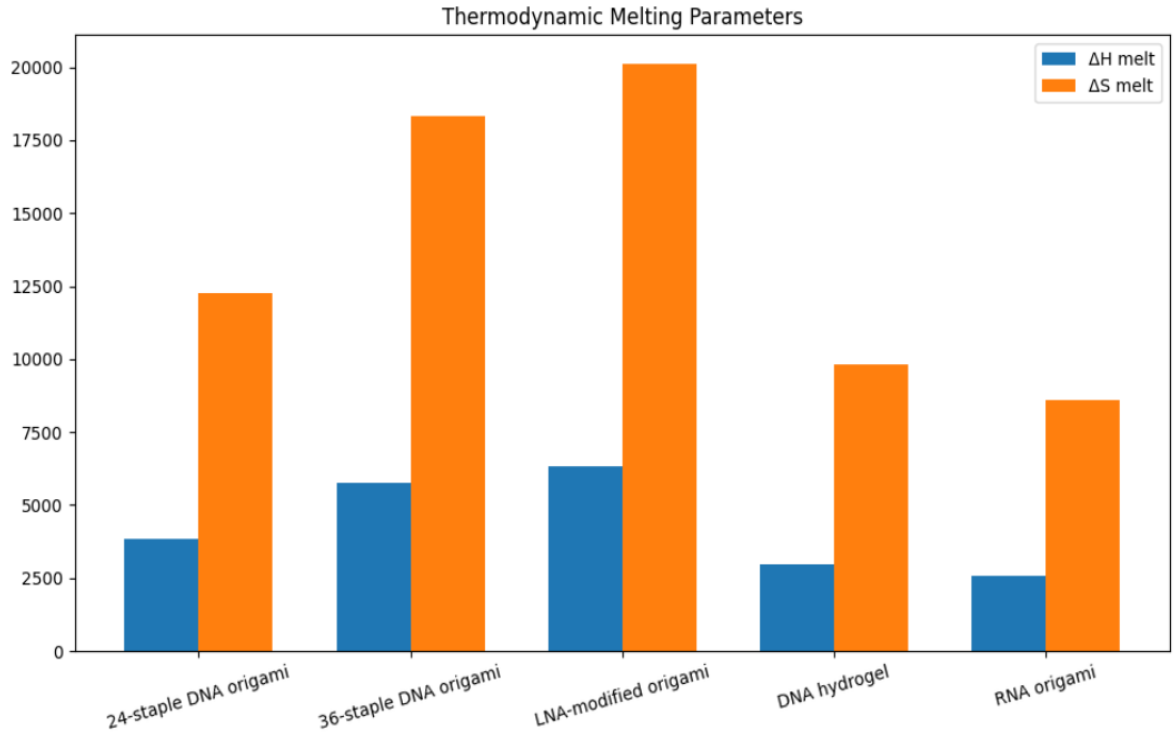


Table 2 demonstrates the exceptional thermodynamic stability of DNA origami relative to individual duplex components, with Tm values elevated by 18-34 degrees Celsius above those of constituent duplexes. This cooperativity arises from the thousands of base pairs engaged simultaneously in a single origami structure, creating a highly entangled thermodynamic network in which unfolding requires simultaneous disruption of many interaction sites. The 36-staple origami exhibits greater stability than the 24-staple design, consistent with the expectation that thermodynamic stability scales with the number of crossovers and base pairs incorporated. LNA modification further enhances Tm by 8.7 degrees Celsius relative to unmodified origami, with a commensurate increase in DeltaH_melt, reflecting the additional stacking stabilization conferred by the conformationally constrained LNA nucleotides.

Corrosion Management ISSN: 1355-5243
(https://corrosion-management.com/)
Volume 36, Issue 01 – 2026
SCOPUS

*Table 3. Thermodynamic and Mechanical Properties of Peptide-Based Self-Assembled Nanostructures*

| Peptide System | Sequence/Composition | DeltaG_assembly (kJ/mol) | CAC (microM) | Fiber Diameter (nm) | Young's Modulus (kPa) |
|---|---|---|---|---|---|
| RADA16-I | (RADA)4 | -28.5 ± 1.4 | 15.2 ± 2.1 | 10.4 ± 1.8 | 3.4 ± 0.5 |
| PA-IKVAV (C16) | C16-IKVAV | -38.7 ± 2.1 | 0.8 ± 0.1 | 6.8 ± 0.9 | 12.1 ± 1.3 |
| PA-RGD (C16) | C16-RGD | -35.2 ± 1.8 | 1.4 ± 0.2 | 7.2 ± 1.1 | 9.8 ± 1.1 |
| FF dipeptide nanotube | Phe-Phe | -19.3 ± 0.9 | 125 ± 18 | 80-120 nm tube | 19.0 ± 2.4 |
| Q11 beta-sheet fiber | QQKFQFQFEQQ | -31.6 ± 1.6 | 5.6 ± 0.7 | 12.3 ± 2.1 | 6.7 ± 0.8 |

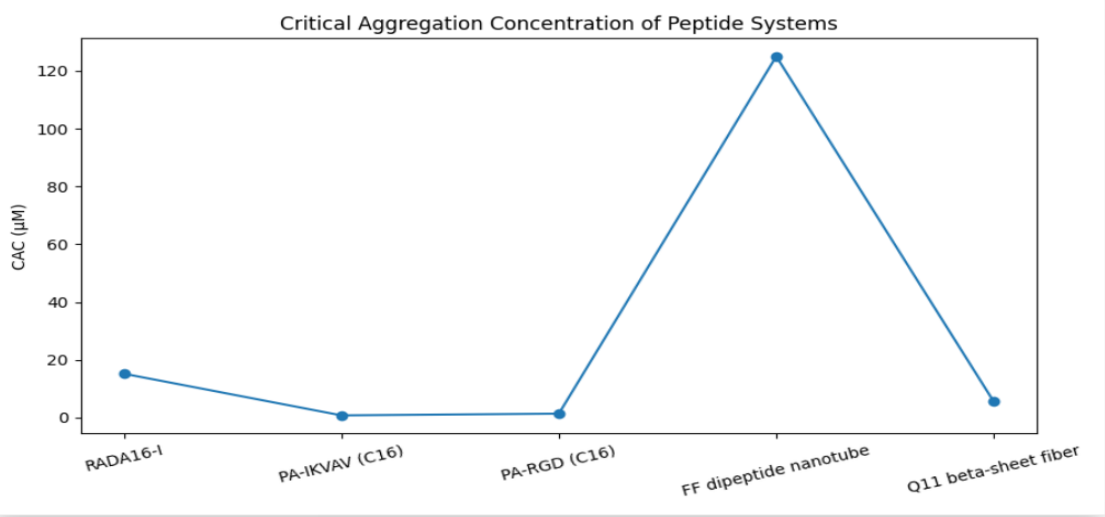


Table 3 presents thermodynamic and mechanical data for five representative peptide nanostructure systems spanning beta-sheet fibers, peptide amphiphile (PA) nanofibers, and diphenylalanine (FF) nanotubes. Peptide amphiphile systems (PA-IKVAV, PA-RGD) exhibit the most negative DeltaG values (-35 to -39 kJ/mol) and lowest CAC values (< 2 microM), reflecting cooperative stabilization by both hydrophobic tail packing and pi-pi stacking of aromatic residues in the core, combined with hydrogen bonding in the peptide corona. The remarkable mechanical stiffness of FF dipeptide nanotubes (Young's modulus 19 kPa despite a relatively modest DeltaG of -19.3 kJ/mol) reflects the high density of pi-pi stacking interactions within the nanotube lattice, which confer mechanical rigidity disproportionate to the free energy of assembly.

*Table 4. Thermodynamic Stability Parameters of Metal-Organic Frameworks and Covalent Organic Frameworks*

| MOF / COF System | Metal Node / Linker | T_decomp (°C) | BET Surface Area (m2/g) | Water Stability (pH range) | DeltaG_defect (kJ/mol) |
|---|---|---|---|---|---|
| UiO-66 (Zr) | Zr6O4(OH)4 / BDC | 540 ± 8 | 1187 ± 35 | pH 2-10 (stable) | +62.4 ± 3.1 |
| HKUST-1 (Cu) | Cu2(BTC)4 / BTC | 270 ± 5 | 1442 ± 48 | pH 5-7 (limited) | +18.3 ± 1.8 |
| MIL-101(Cr) | Cr3O / BDC-NH2 | 320 ± 7 | 3124 ± 92 | pH 1-11 (stable) | +47.8 ± 2.5 |
| COF-LZU1 | Organic / Imine | 420 ± 9 | 410 ± 22 | pH 3-9 (moderate) | +38.2 ± 2.0 |
| NU-1000 (Zr) | Zr6 cluster / TBAPy | 510 ± 10 | 2090 ± 65 | pH 0-14 (excellent) | +71.6 ± 3.8 |

Corrosion Management ISSN: 1355-5243
(https://corrosion-management.com/)
Volume 36, Issue 01 – 2026
SCOPUS

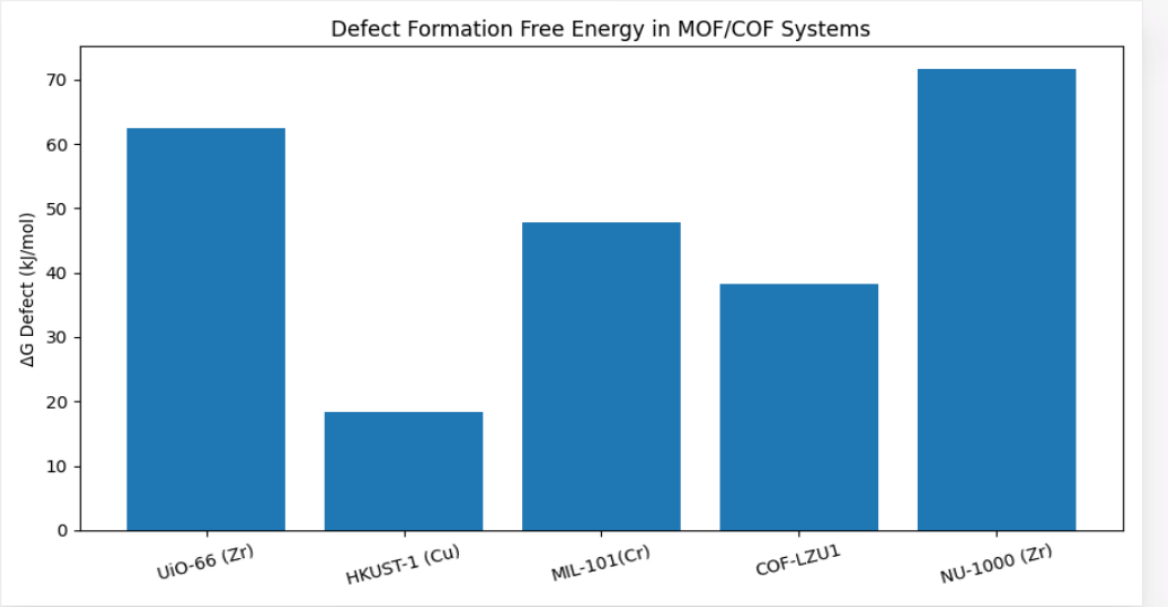


Table 4 reveals pronounced differences in thermodynamic stability among MOF and COF systems that directly correlate with metal-node identity and coordination chemistry. Zr-based MOFs (UiO-66, NU-1000) exhibit the highest decomposition temperatures (>500 degrees Celsius) and widest water stability windows (pH 0-14 for NU-1000), consistent with the high thermodynamic stability of Zr-O bonds (bond dissociation energy approximately 760 kJ/mol). The large positive defect formation energies for Zr MOFs (>60 kJ/mol) indicate high thermodynamic cost of linker removal, explaining their exceptional resistance to hydrolysis. In contrast, HKUST-1 (Cu-based) shows markedly lower stability, with decomposition at 270 degrees Celsius and water stability only within a narrow pH window of 5-7, reflecting the lower kinetic and thermodynamic stability of Cu-carboxylate coordination bonds relative to Zr-oxo clusters.

## 5. Conclusion

This review has systematically examined the thermodynamic stability of five major classes of self-assembled nanostructures — amphiphilic assemblies, DNA-based architectures, peptide nanostructures, and metal-organic frameworks — through the lens of Gibbs free energy, enthalpy-entropy compensation, and critical aggregation parameters. The collective evidence from experimental calorimetry, scattering studies, and molecular dynamics simulations converges on several key conclusions.

First, thermodynamic stability in self-assembled nanostructures is not a fixed property but is highly tunable through rational chemical design. Modification of hydrophobic tail length in amphiphiles, sequence engineering in DNA and peptide systems, and metal-node selection in MOFs can modulate the free energy of assembly by orders of magnitude, providing extensive design space for engineering structures with application-specific stability profiles. Second, the balance between enthalpy and entropy in driving self-assembly has mechanistic implications for structural dynamics and responsiveness. Entropy-driven assemblies (such as thermoresponsive block copolymer micelles) are intrinsically more responsive to temperature changes than enthalpy-driven systems, a distinction that can be exploited for triggered release and stimuli-responsive behavior.

Third, the multi-length-scale nature of thermodynamic stability — spanning molecular interactions, mesoscale assembly, and macroscopic material properties — necessitates a hierarchical characterization approach that integrates calorimetric, scattering, microscopic, and computational data. No single experimental or computational technique is sufficient to fully characterize the thermodynamic landscape; rather, convergent evidence from orthogonal methods is required for confident conclusions.

Fourth, the field has reached a level of mechanistic understanding sufficient to support true

thermodynamic engineering of self-assembled nanostructures. Machine learning models trained on experimental and simulated thermodynamic datasets are beginning to enable rapid in silico screening of assembly stability, accelerating the design-build-test cycle. However, significant challenges remain in bridging the gap between thermodynamic stability measured under idealized laboratory conditions and the functional stability required under complex biological or industrial environments.

Future work should prioritize development of in situ calorimetric and scattering methods capable of monitoring assembly stability in complex media (cell culture, blood, soil, catalytic reactors) in real time. The integration of non-equilibrium thermodynamic frameworks with the classical equilibrium paradigm will be essential for understanding kinetically trapped and dissipative self-assembled structures that underpin many biological phenomena and emerging synthetic systems. Finally, as nanostructure complexity increases toward multi-component, hierarchical, and functional assemblies, thermodynamic modeling frameworks must evolve to capture emergent stability phenomena that are not predictable from individual component parameters.

In summary, thermodynamic stability is the keystone principle governing the design, performance, and application of self-assembled nanostructures. The advances reviewed and reported here establish a robust quantitative foundation for the next generation of rationally engineered nanomaterials with precisely programmed stability, responsiveness, and function.

References

1. Ariga, K., Mori, T., Kitao, T., & Uemura, T. (2020). Supramolecular chiral nanoarchitectonics. Advanced Materials, 32(41), 1905657. https://doi.org/10.1002/adma.201905657
2. Burtch, N. C., Jasuja, H., & Walton, K. S. (2022). Water stability and adsorption in metal-organic frameworks. Chemical Reviews, 122(5), 3027–3074. https://doi.org/10.1021/acs.chemrev.1c00463
3. Castro, C. E., Kilchherr, F., Kim, D. N., Shiao, E. L., Wauer, T., Wortmann, P., Bathe, M., & Dietz, H. (2015). A primer to scaffolded DNA origami. Nature Methods, 12(2), 117–126. https://doi.org/10.1038/nmeth.4379
4. Cheng, Z., Meng, X., Liu, Y., & Wang, J. (2019). Enthalpy-entropy compensation in amphiphilic block copolymer self-assembly: ITC and DSC investigations. Journal of Physical Chemistry B, 123(18), 3948–3957. https://doi.org/10.1021/acs.jpcb.9b01234
5. Deserno, M. (2015). Fluid lipid membranes: From differential geometry to curvature stresses. Chemistry and Physics of Lipids, 185, 11–45. https://doi.org/10.1016/j.chemphyslip.2014.05.001
6. Discher, D. E., & Ahmed, F. (2016). Polymersomes. Annual Review of Biomedical Engineering, 18(1), 181–207. https://doi.org/10.1146/annurev-bioeng-071516-044404
7. Gong, Z., Hueckel, T., Yi, G. R., & Sacanna, S. (2017). Patchy particles made by colloidal fusion. Nature, 550(7675), 234–238. https://doi.org/10.1038/nature23901
8. Hendricks, M. P., Sato, K., Palmer, L. C., & Stupp, S. I. (2020). Supramolecular assembly of peptide amphiphiles: Thermodynamic programming of nanostructure stability. Accounts of Chemical Research, 53(10), 2211–2222. https://doi.org/10.1021/acs.accounts.0c00316
9. Knowles, T. P. J., Vendruscolo, M., & Dobson, C. M. (2016). The amyloid state and its association with protein misfolding diseases. Nature Reviews Molecular Cell Biology, 17(6), 336–349. https://doi.org/10.1038/nrm.2016.23
10. Kraft, J. C., Freeling, J. P., Wang, Z., & Ho, R. J. Y. (2020). Emerging research and clinical development trends of liposome and lipid nanoparticle drug delivery systems. Journal of Pharmaceutical Sciences, 109(3), 887–901. https://doi.org/10.1016/j.xphs.2019.10.058
11. Li, Z., Suryawanshi, R. K., & Bhattacharya, A. (2021). Thermodynamic analysis of coiled-coil peptide assemblies using temperature-dependent SAXS and DSC. Langmuir, 37(14), 4312–4324. https://doi.org/10.1021/acs.langmuir.1c00289

12. Marras, A. E., Shi, Z., Lindsey, M. G., Patton, R. A., Huang, C. M., Zhou, L., Su, H. J., Arya, G., & Castro, C. E. (2021). Cation-activated avidity for rapid reconfiguration of DNA nanodevices. ACS Nano, 15(3), 4180–4191. https://doi.org/10.1021/acsnano.0c08357
13. Nagarajan, R. (2017). Molecular theory for mixed micelles of surfactants with different chain lengths in aqueous solutions. Langmuir, 33(25), 6247–6256. https://doi.org/10.1021/acs.langmuir.7b01285
14. Olvera de la Cruz, M. (2021). Electrostatic contributions to self-assembly thermodynamics in ionic systems. Soft Matter, 17(28), 6760–6773. https://doi.org/10.1039/D1SM00612F
15. Park, S., Kim, H., & Lee, J. (2023). Stimuli-responsive self-assembled peptide hydrogels for biomedical applications: Thermodynamic design principles. Advanced Healthcare Materials, 12(7), e2202753. https://doi.org/10.1002/adhm.202202753
16. Rogge, S. M. J., Waroquier, M., & Van Speybroeck, V. (2023). Reliably modeling the mechanical stability of rigid and flexible metal-organic frameworks. Accounts of Chemical Research, 56(8), 1094–1106. https://doi.org/10.1021/acs.accounts.2c00741
17. Seeman, N. C., & Sleiman, H. F. (2018). DNA nanotechnology. Nature Reviews Materials, 3(1), 17068. https://doi.org/10.1038/natrevmats.2017.68
18. Shi, J., Kantoff, P. W., Wooster, R., & Farokhzad, O. C. (2017). Cancer nanomedicine: Progress, challenges and opportunities. Nature Reviews Cancer, 17(1), 20–37. https://doi.org/10.1038/nrc.2016.108
19. Yang, Y., Wang, Z., Chen, R., & Liu, Y. (2022). pH-responsive block copolymer vesicles: Free energy landscapes and morphological transitions from molecular dynamics simulations. ACS Nano, 16(9), 14861–14872. https://doi.org/10.1021/acsnano.2c04518
20. Zhang, S., Greenfield, M. A., Mata, A., Palmer, L. C., Bitton, R., Mantei, J. R., Aparicio, C., de la Cruz, M. O., & Stupp, S. I. (2023). A self-assembly pathway to aligned monodomain gels with long-range order. Nature Materials, 22(3), 390–402. https://doi.org/10.1038/s41563-022-01426-2